

Differential Scanning Calorimetric Study of 6OCB Liquid Crystal using Logger Pro

Laura Elizabeth Byrne¹ and Dipti Sharma^{2*}

¹Undergraduate student, Emmanuel College, Boston, MA, USA

²supervisor Emmanuel College, Boston, MA, USA,

*Corresponding author: Dipti Sharma, supervisor Emmanuel College, Boston, MA, USA.

Submitted: 20 Aug 2023

Accepted: 25 Aug 2023

Published: 31 Aug 2023

Citation: Laura Elizabeth Byrne and Dipti Sharma (2023). Differential Scanning Calorimetric Study of 6OCB Liquid Crystal using Logger Pro, *J of Physics & Chemistry 1(1)*., 01-11.

Abstract

This study explores the thermal behavior and properties of the 4-cyano-4'-hexyloxybiphenyl (6OCB) liquid crystal as it undergoes different phase transitions. The liquid crystal was run in Differential Scanning Calorimetry (DSC), where the sample of 6OCB was heated from -40 °C to 100 °C and then cooled from 100 °C to -40 °C at a rate of 20 °C/min. Logger Pro was used to analyze the data and compare it with the details of other liquid crystals from the n-alkyloxy-cyanobiphenyl (nOCB) family as well as the n-alkyl-cyanobiphenyl (nCB) family, in order to see how tail length and the presence of oxygen affect phase transitions. The sample of 6OCB showed unique behavior as it was cooled, forming a multipeak that was analyzed using Gaussian Analysis. It was found that 6OCB has a wide nematic range during cooling, suggesting that it could be useful in liquid crystal displays (LCD) on devices that may be used in warmer environments.

Keywords: Liquid Crystal, Differential Scanning Calorimetry, 6OCB, LCD, States of Matter, Crystalline, Nematic, Isotropic, Thermodynamics, Specific Heat Capacity, Logger Pro, Endothermic, Exothermic, Enthalpy, Gaussian Analysis, Phase Transition, Multipeak Analysis.

Introduction

Differential Scanning Calorimetry (DSC) is a technique used to analyze the properties of samples using an analytical instrument that heats and cools the sample while measuring the temperature and heat flow. Most DSC instruments have two compartments in which the sample and reference material are placed and heated at the same time. The instrument keeps the sample and reference at the same temperatures, so if the sample begins to undergo an endothermic or exothermic change, more or less heat will be needed to change its temperature at the same rate as the reference material. Using this method, the state of the material can be detected in terms of phase transitions of the sample and can be analyzed further for heat capacity and enthalpy details. The DSC is an advantageous technique due to the speed, sensitivity, and accuracy of the instrument, as well as the need for only a small amount of the sample material which requires little preparation to obtain results [1-4].

DSC can be utilized for a variety of research. For example, when studying the properties of polymers, it is important to know the temperature at which these substances melt or crystallize. Furthermore, this technique can be used to analyze proteins and determine the enthalpy of denaturation. [1-4] DSC is also useful in analyzing the properties of Liquid Crystals (LCs), due to their unique phase changes. While typical matter can only exist in the three states known as solid, liquid, and gas, LCs often have

more than three phases. Some examples of LC phases are crystalline, smectic, nematic, and isotropic. These phases depend on the orientation and position of the molecules, which lose their structure and order as they go from crystalline to isotropic. In the crystalline state, the molecules are ordered and densely packed in rows and columns, all facing the same direction. After the crystalline state, some LCs reach the smectic phase where they lose some of the even spacing of the crystalline state by forming clusters, but generally remain in rows. The molecules then lose more order when reaching the nematic state, between liquid and crystal, which gives the substance its name. In this state, the molecules point generally in the same direction but are not layered and form small groups. Once the LC reaches the isotropic state, the molecules have lost all order and the substance is fully liquid. Thermotropic liquid crystals will change phases depending on the temperature range, and can change orientation due to electrical current, which makes them beneficial and effective for technological uses such as Liquid Crystal Displays (LCDs) [5-13].

LCDs utilize liquid crystals mostly in the nematic phase to display images on a screen, such as a smart phone, television, or laptop. In LCDs, a thin film of liquid crystal is spread between two panels which are located in front of a backlight. The unique phase properties of liquid crystals allow for the orientation of their molecules to be manipulated to let through different colors

of pixels, which in turn create an image when passing through layers of filters. Due to their effectiveness and practicality, LCDs have widely replaced the use of cathode-ray tube (CRT) technology, which requires large, bulky parts and lots of power. LCDs only require a few thin layers of material, which allows for thinner, lighter technology [14-19]. In the past, 8CB was the focus of most LC research, but in 1972, 5CB was synthesized at the University of Hull, and it was discovered by Professor George Gray that 5CB exhibited properties that could be used for LCD [20-21]. Both 8CB and 5CB belong to the same family of LCs known as n-alkyl-cyanobiphenyl (nCB).

Extensive research has been done on nCB LCs; thus, our interest is to use a different family of LC to see if any significant results and properties can be found relevant to LCDs. One of the other families of LCs is n-alkoxy-cyanobiphenyl (nOCB). In this family, “n” represents the tail made up of C-C bonds, “CB” represents the body, and “O” is the oxygen that connects the tail and the body. While nCB and nOCB LCs have almost identical structures, in nCB there is no oxygen in between the tail and body of the molecule. For both, however, as the number of “n” increases, the length of the tail increases. The tail length in these families of LCs can greatly affect the properties and behavior, including its phase transition temperatures. Since nCB has been widely studied, including 5CB and 8CB, the molecule of interest in this study is 4-cyano-4'-hexyloxybiphenyl (6OCB), a liquid crystal from the nOCB family where $n = 6$, meaning it has a tail length comparatively between that of 5CB and 8CB, and the same length as 6CB [21-22].

Material, Experimental Details and Theory

This research is performed with Bulk 4-hexyl-oxy-4'-cyanobiphenyl (6OCB) Liquid Crystal (LC), also referred to as 4-cyano-4'-hexyloxybiphenyl. The molecular formula of 6OCB is $C_{19}H_{21}NO$, and it is solid at room temperature. The sample of 6OCB LC was used in a Differential Scanning Calorimetry (DSC) model MDSC 2920 from TA instruments at WPI to study its thermal behavior and phase transitions to find unique details that could make 6OCB important in research and technology. Furthermore, our interest is to see how 6OCB differs from 6CB as well as other members of nOCB.

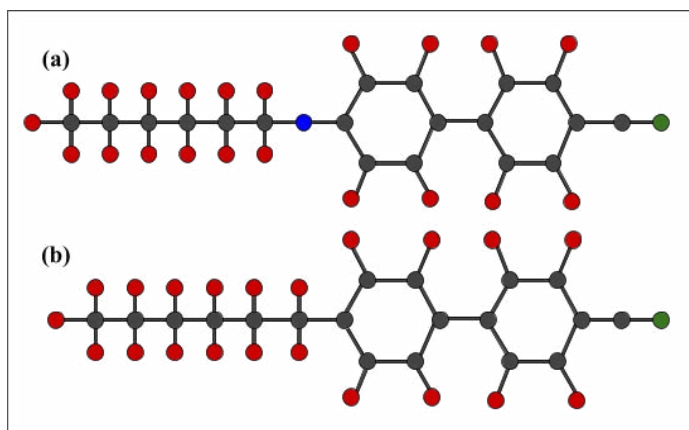


Figure 1: The Molecular Structures Of (A) 6ocb and (b) 6CB.

Figure 1 shows the molecular structures of the liquid crystals 6OCB and 6CB. This diagram shows the similarities between the nOCB and nCB families, which share the same basic structure with the exception of the oxygen, depicted by the blue circle. It can be seen that 6CB is missing an oxygen atom, and instead its carbon chain connects directly to the ring.

The detailed skeletal structure of 6OCB is depicted in Figure 2, where the structure on the left shows a full chain of six carbons. The structure on the right shows the more condensed structure, labeling the atoms that are in the tail. “CN” represents the cyano group which consists of a carbon atom triple-bonded to a nitrogen atom.

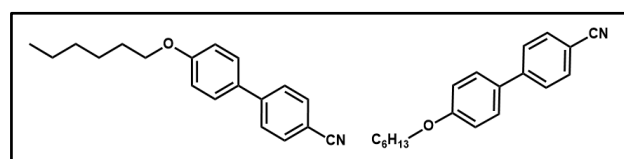


Figure 2: Molecular Structure of 6OCB.

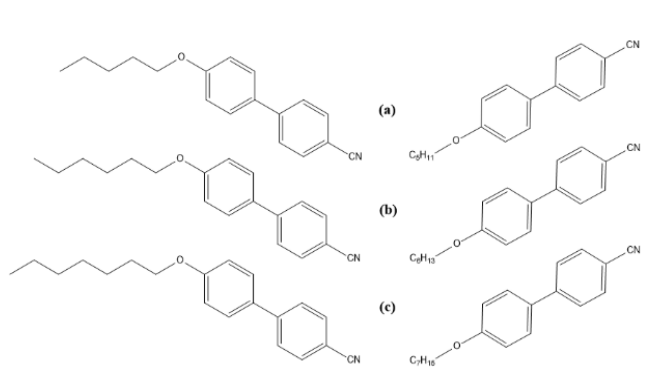


Figure 3: Molecular Structures of (a) 5OCB, (b) 6OCB, and (c) 7OCB.

Figure 3 shows a comparison between the molecular structures of 5OCB, 6OCB, and 7OCB. It can be seen that 5OCB and 7OCB are odd molecules with an odd number of CH groups in the chain. Due to this similarity, they end in the same direction, whereas 6OCB is an even molecule with an even number of carbons, and ends in the opposite direction of the odd molecules 5OCB and 7OCB. Our interest is to pick an even nOCB molecule to see if it can show some difference in its thermal properties than 5OCB and 6CB.

For the experimental portion of this study, the bulk sample of 4-cyano-4'-hexyloxybiphenyl (6OCB), with a molecular weight of 279.38 g/mol, was placed in the DSC instrument to study its thermal and phase transition details. For calorimetric experiments, a small amount of 6OCB was loaded into pans, sealed with lids using a DSC press, and then placed inside a DSC instrument. The heating and cooling of the 6OCB is done from $-40\text{ }^{\circ}\text{C}$ to $100\text{ }^{\circ}\text{C}$ and from $100\text{ }^{\circ}\text{C}$ to $-40\text{ }^{\circ}\text{C}$ at a constant heating and cooling rate of $20\text{ }^{\circ}\text{C}/\text{min}$. The respective heat flow of the samples was recorded along with temperature and time change during the heating and cooling scans.

DSC results show that when 6OCB is heated, it forms one large endothermic peak and one small endothermic peak on heating, and then a small exothermic peak, and a large exothermic peak with multiple small peaks in cooling. These peaks correspond to a Crystalline to Nematic peak, K-N (large peak) and a Nematic to Isotropic peak, N-I (small peak) on heating and cooling. The detailed thermal analysis of 6OCB can reveal the facts of molecular arrangements and alignments during these phase transitions in 6OCB. The DSC data was then analyzed by Logger pro to see more clear results.

These thermal peaks are indications of a change of state of the 6OCB material while it is heated and cooled. While 6OCB is heated, the molecular arrangement of 6OCB changes from Crystalline to Nematic, and then, when it is fully melted, to Isotropic. When it is cooled, its state changes from Isotropic to Nematic and then to Crystalline. The typical alignment of molecules during each of these phases is shown by Figure 4.

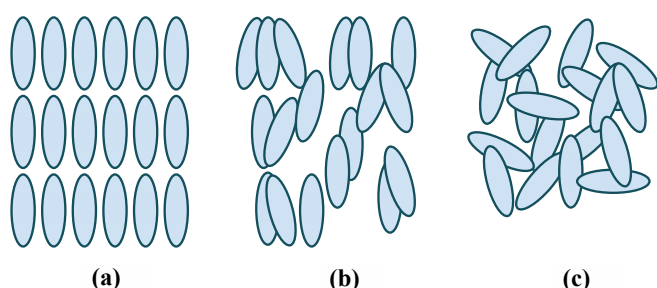


Figure 4: Arrangement Of 6ocb Molecules in the (A) Crystalline, (B) Nematic, And (C) Isotropic Phases.

The theory used in DSC for 6OCB liquid crystal can be shown as given below.

When DSC is used, a transfer of energy takes place to heat and cool the sample. When 6OCB is heated, energy, as heat, is absorbed. When the sample is cooled, the heat is released. This heat can be given as (Q), which relates to the mass of the 6OCB (m), specific heat of capacity (Cp), and temperature change (ΔT) as

$$Q = m \cdot C_p \cdot \Delta T \quad \text{--- 1}$$

In DSC, the heat flow is recorded as a function of temperature and can be written where dQ/dt is heat flow and dT/dt is the ramp rate,

$$dQ/dt = m \cdot C_p \cdot dT/dt \quad \text{--- 2}$$

Specific heat capacity of the 6OCB can be given as

$$C_p = (1/m) \cdot [(dQ/dt)/(dT/dt)] \quad \text{--- 3}$$

The heat energy involved in heating and cooling for each transition is the Enthalpy (ΔH), and can be given as the area under the peak, found by integrating the peak of the graph plotted for Cp versus T as shown in the equation 3.

$$\Delta H = \int C_p \cdot dT = (1/m) \int (dQ/dt) \cdot dt \quad \text{--- 4}$$

Gaussian Analysis

Gaussian analysis is used in order to analyze the unique peaks formed by the DSC data. The Gaussian equation is written as follows

$$f(x) = a \exp \left[-\frac{(x-b)^2}{2c^2} \right] + d \quad \text{--- 5}$$

The constant (a) represents the height of the peak, while (b) is the position of the peak's center. The constant (c) represents the width of the peak, and (d) is the asymptote of the peak. The following papers report more details on Gaussian analysis [22-23].

Results

The details of 6OCB and its phase transitions are studied using DSC and analyzed using Logger pro. These details can be seen in the results section below in the form of figures. Figure 5 depicts the heating and cooling of the sample of 6OCB between around -15 °C and 100 °C, using the data from DSC. In the beginning, as the material is heated the plot is rather flat, but starts to lose stability as it approaches 50 °C. A significant and smooth endothermic peak appears at 59.55 °C, where the material is transitioning from crystalline to nematic, as well as a smaller endothermic peak at 76.92 °C, where the material is going from nematic to isotropic. As the material is cooled, a small exothermic peak appears at 73.94 °C, where the material is transitioning back to the nematic state. After this peak, the plot remains relatively steady until three combined exothermic peaks appear at 26.00 °C, 22.54 °C, and 18.67 °C, when the material is crystallizing.

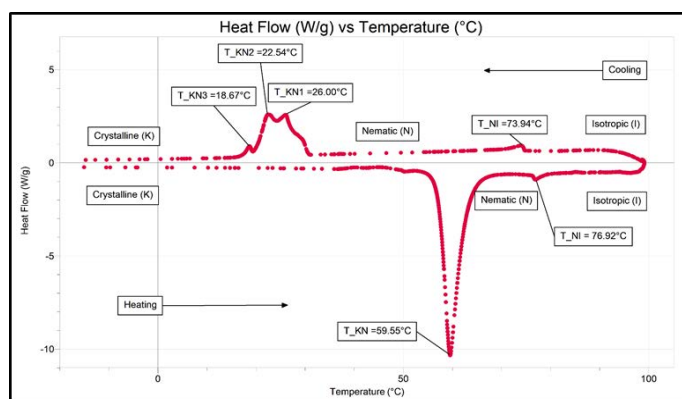


Figure 5: Heat Flow, Hf (W/G) Vs Temperature, T (°C) Of 6ocb Being Heated from Crystalline to Nematic, Then to Isotropic, and Then Being Cooled from Isotropic to Nematic, Then to Crystalline Using Dsc.

Using the data recorded by DSC, the specific heat capacity at each recorded temperature was calculated and plotted in Figure 6. The integral of this plot, shown in pink, represents the thermal energy that is used by 6OCB as it is being heated and cooled. The downward-facing endothermic peaks show where the LC is absorbing energy, while the upward-facing exothermic peaks show where the LC is releasing energy. The overall change in internal energy was found to be 454.5 J/g using Logger Pro. Additionally, it can be seen that the energy involved is greater in the crystalline-nematic phase transitions, both marked T_KN, than in the nematic-isotropic phase transitions, marked T_NI.

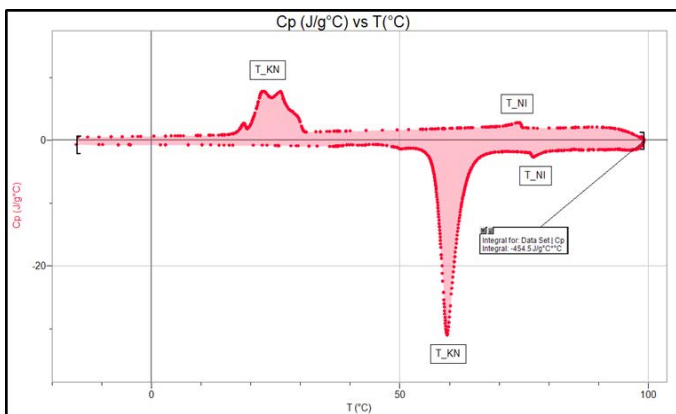


Figure 6: Specific Heat Capacity, C_p ($J/g^{\circ}C$) Vs Temperature, T ($^{\circ}C$) Of 6ocb Being Heated and Cooled. The Pink Shaded Area Shows the Change in Internal Energy of 6OCB.

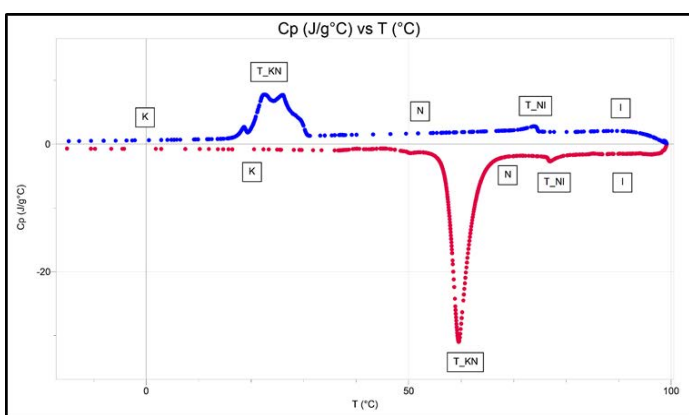


Figure 7: C_p ($J/g^{\circ}C$) vs T ($^{\circ}C$) of 6OCB Being Heated (In Red) and Cooled (in Blue).

Figure 7 more clearly shows the heating and cooling of 6OCB, distinguishing one from the other with red data points depicting heating, while the blue data points show cooling. It can be noticed that the crystalline (K) to nematic (N) transition, labeled T_{KN} , occurs at different temperatures depending on whether the LC is being heated or cooled. However, the nematic to isotropic (I) transition, labeled T_{NI} , occurs within a similar temperature range. This means that the sample remains in the nematic phase longer when being cooled.

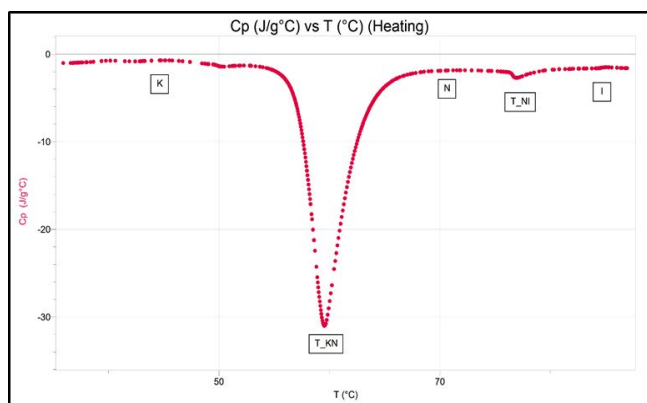


Figure 8: Zoomed-In Graph of C_p ($J/G^{\circ}C$) Vs T ($^{\circ}C$) Of 6ocb Being Heated from Crystalline (K) To Nematic (N) and then to Isotropic (I), Between $30^{\circ}C$ and $90^{\circ}C$.

Focusing on only the heating of the sample, in Figure 8 it can be seen that the liquid crystal begins in the crystalline state, but as the temperature rises further, the heat capacity becomes more negative and reaches a peak, shown by T_{KN} . At this point, the sample is half crystalline and half nematic. As the temperature increases, the percent of nematic sample increases until it is fully nematic. The plot briefly remains steady until the heat capacity begins to decline once again, forming the small peak labeled T_{NI} , where the sample is half nematic and half isotropic. The heat capacity increases as the crystal enters the isotropic state. The significant difference in size of the peaks indicates that the K-N transition resulted in a larger change in energy than the N-I transition.

The magnified plot of the cooling of 6OCB, seen in Figure 9, shows an overall decline of the specific heat capacity as the temperature approaches zero, with the exception of the peaks at which the phase transitions are occurring. The sample is cooled from its isotropic state, reaching a phase transition at T_{NI} , and remaining in the nematic state until the next exothermic curve with three peaks, labeled T_{KN1} , T_{KN2} , and T_{KN3} . This indicates that parts of the sample had undergone the phase transition at different times.

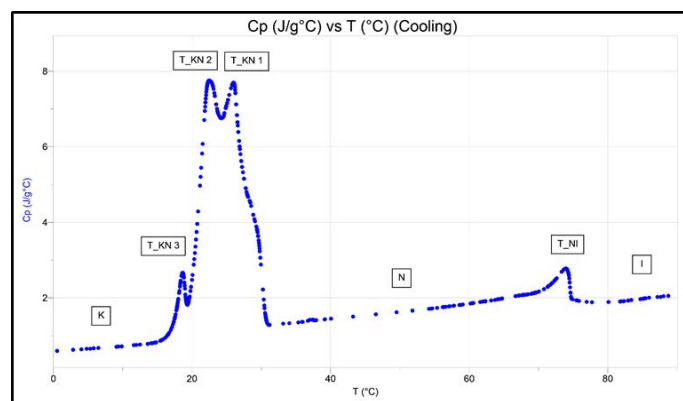


Figure 9: Zoomed-In Graph of C_p ($J/G^{\circ}C$) Vs T ($^{\circ}C$) Of 6ocb Being Cooled from Isotropic (I) To Nematic (N) To Crystalline (K) Between $0^{\circ}C$ and $90^{\circ}C$.

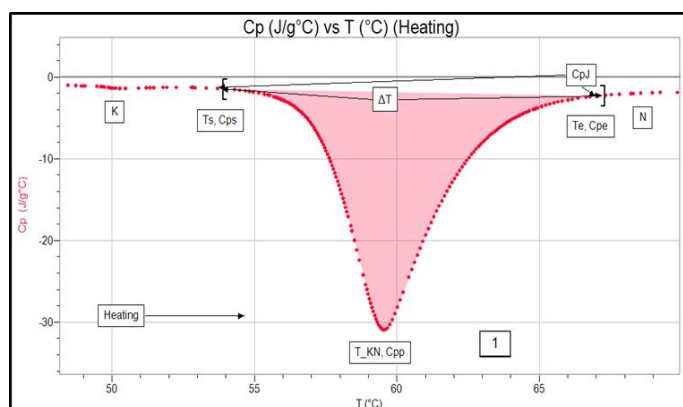


Figure 10: C_p ($j/g^{\circ}C$) vs t ($^{\circ}C$) of 6ocb Being Heated from Crystalline (k) to Nematic (n). The Pink Shaded Area Shows the Integral of the Peak.

The further magnified plot, seen in Figure 10, shows the first endothermic peak (T_{KN}) that appears during the heating

of 6OCB, which is the transition from crystalline to nematic. Peak integration reveals the enthalpy of the phase transition, which was calculated to be 159.77 J/g using Logger Pro. This represents how much thermal energy is involved and absorbed in the K-N phase transition, changing the sample's internal energy. In Figures 10-16, T_s and T_e mark the beginning and end temperatures of the phase transition, and ΔT shows the overall change in temperature. C_{ps} and C_{pe} mark the beginning and end specific heat capacities, while C_{pp} marks the specific heat capacity at the peak. C_{pJ} represents the wing jump of the peak.

The next endothermic peak can be seen in Figure 11, where the sample of 6OCB is transitioning from nematic to isotropic. The enthalpy of this phase transition was found to be 29.33 J/g, which is the thermal energy absorbed during the N-I transition, and is depicted by the pink shaded area. This value is much less than that of the K-N transition, because when the molecules are in the crystalline phase, more energy is required to break the crystal lattice formation. When the sample is in the nematic phase, the crystal lattice is already broken, thus it requires less energy to transition to isotropic. Additionally, there is a noticeable wing jump, due to the magnified scale, as the heat capacity of the sample is lower on average when it is in the nematic phase, but higher in the isotropic phase. This graph also shows the details of when the N-I transition starts and ends, as well as the height and width of the N-I peak.

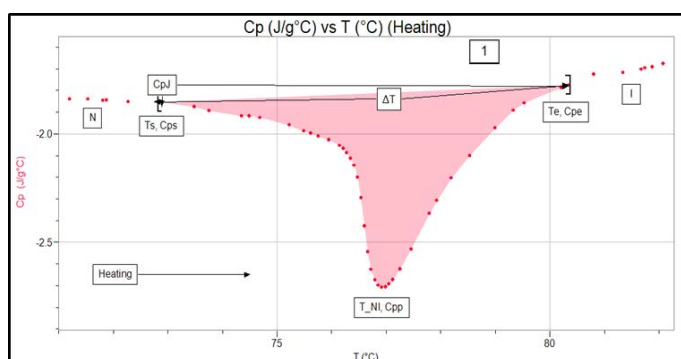


Figure 11: C_p (J/g°C) vs T (°C) of 6OCB Being Heated from Nematic (N) to Isotropic (I). The Pink Shaded Area Shows the Integral of the Peak.

Figure 12 depicts the magnified plot of the exothermic phase transition from nematic to isotropic as 6OCB is cooled. The enthalpy of this I-N peak, shown by the blue shaded area, was calculated to be 33.07 J/g, and represents the amount of thermal energy that is released from the liquid crystal as its temperature is lowering. This value is similar to the amount of energy that was originally absorbed during the N-I transition, seen in Figure 11. Furthermore, much like the N-I transition, there is a noticeable wing jump in this peak, as the specific heat capacity on average is higher in the nematic state than in the isotropic state.

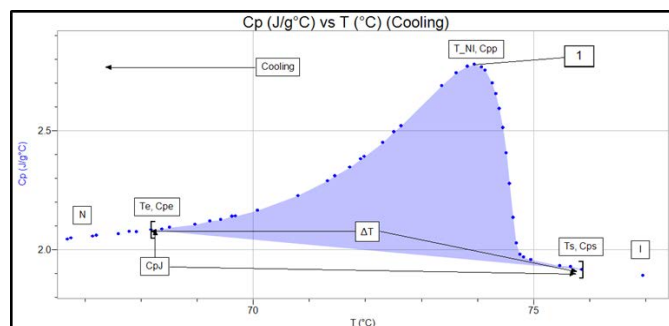


Figure 12: C_p (J/g°C) vs T (°C) of 6OCB Being Cooled from Isotropic (I) to Nematic (N). The Blue Shaded Area Shows the Integral of the Peak.

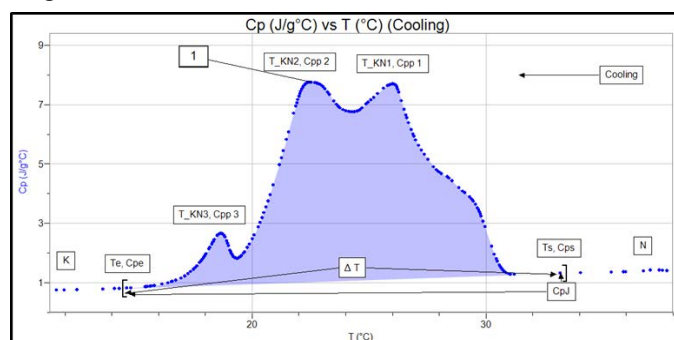


Figure 13: C_p (J/g°C) vs T (°C) of 6OCB Being Cooled from Nematic (N) to Crystalline (K). The Blue Shaded Area Shows the Integral of the Peak.

The second exothermic phase transition of the sample from nematic to crystalline can be seen in Figure 13. The enthalpy of this curve, shown by the blue shaded area, was found to be 91.89 J/g, which is the amount of internal energy that is lost by the sample as it undergoes the N-K transition. More energy is released during this phase transition than during the I-N transition. Unlike the previous phase transitions, which each show one relatively smooth peak, the N-K cooling curve shows multipeaks. There are three defined multipeaks, indicating three separate stages of transition within the sample of the LC.

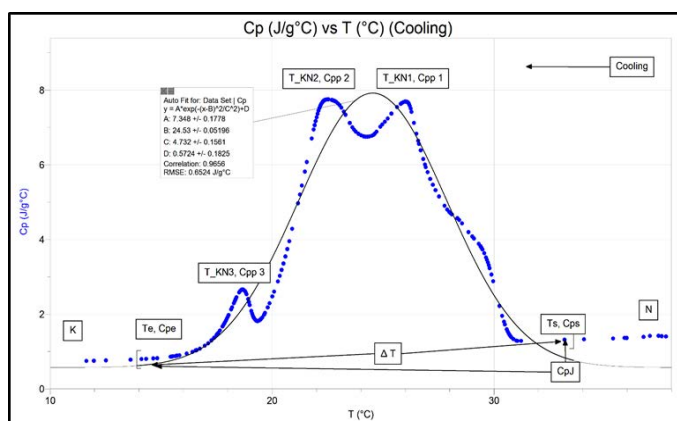


Figure 14: Single Gaussian Curve Fit Of 6ocb Being Cooled from Nematic (N) to Crystalline (K) Using the Plot of the C_p (J/g°C) vs T (°C).

In order to more closely examine the unique cooling behavior of 6OCB, Gaussian Analysis is performed for the K-N and N-K

peaks using Logger Pro. First, a single-peaked curve fit was applied to the entirety of the N-K phase transition, as seen in Figure 14. Using this method, the phase transition can be examined as a possible single peak rather than a multipeak. This process follows Gaussian theory, mentioned in the theory section, and uses the Gaussian Equation, which Logger Pro gives as,

$$y = A * \exp(-(x-B)^2/C^2) + D$$

Gaussian Analysis Using Logger Pro for the N-K Transition with One Curve Fit Provided the Following Data.

- A: 7.348 +/- 0.1778
- B: 24.53 +/- 0.05196
- C: 4.732 +/- 0.1561
- D: 0.5724 +/- 0.1825
- Correlation: 0.9656
- RMSE: 0.6524 J/g°C

Next, a separate curve fit was applied to each individual peak using the Gaussian equation for the same N-K phase transition during cooling, as seen in Figure 15, following Gaussian theory. The three Gaussian fits visually seem to match the phase transition more accurately than the single peak, which is also indicated by the correlation values, which are higher in Figure 15 than in Figure 14.

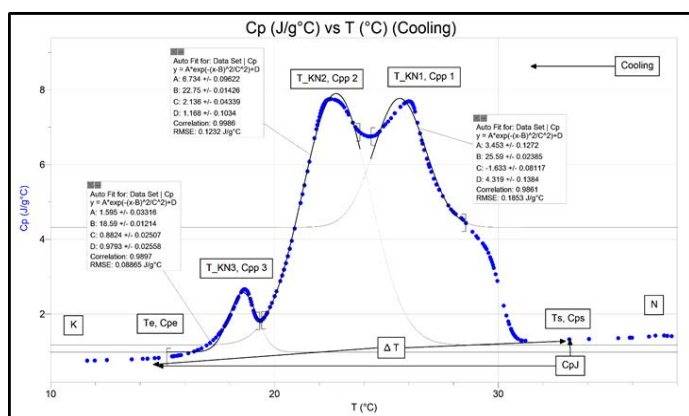


Figure 15: Three Gaussian Curve Fits for Each Separate Peak of the Cp (J/g°C) vs T (°C) Plot of 6OCB Being Cooled from Nematic (N) to Crystalline (K).

Gaussian Analysis of Each Peak Gave the Following Data

Peak T_KN1:

- A: 3.453 +/- 0.1272
- B: 25.59 +/- 0.02385
- C: -1.633 +/- 0.08117
- D: 4.319 +/- 0.1384
- Correlation: 0.9861
- RMSE: 0.1853 J/g°C

Peak T_KN2:

- A: 6.734 +/- 0.09622
- B: 22.75 +/- 0.01426
- C: 2.136 +/- 0.04339
- D: 1.168 +/- 0.1034

- Correlation: 0.9986
- RMSE: 0.1232 J/g°C

Peak T_KN3:

- A: 1.595 +/- 0.03316
- B: 18.59 +/- 0.01214
- C: 0.8824 +/- 0.02507
- D: 0.9793 +/- 0.02558
- Correlation: 0.9897
- RMSE: 0.08865 J/g°C

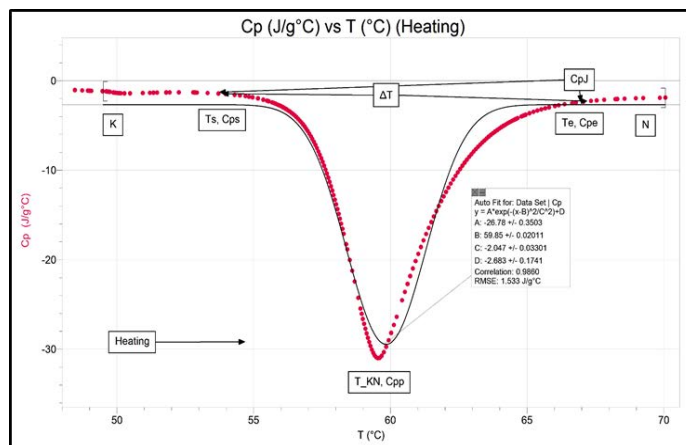


Figure 16: Gaussian Fit of the Cp (J/g°C) vs T (°C) Plot of the Crystalline (K) to Nematic (N) Transition.

This method was also applied to the K-N phase transition that occurs during the heating of 6OCB, as seen in Figure 16. Unlike the N-K cooling phase transition, the plot of the K-N heating transition does not contain any multi-peaks. The Gaussian peak is somewhat close, visually, to the T_KN peak, and shows a relatively high correlation.

The following was provided by Logger Pro using Gaussian analysis

- A: -26.78 +/- 0.3503
- B: 59.85 +/- 0.02011
- C: -2.047 +/- 0.03301
- D: -2.683 +/- 0.1741
- Correlation: 0.9860
- RMSE: 1.533 J/g°C

Figure 17 shows detailed results of 6OCB as it was heated and cooled over a span of nearly 20 minutes. The graph shows the heat flow (W/g) versus time (min), which was recorded by the DSC instrument. The downward peaks show when the sample was being heated, whereas the upward peaks show cooling. From this graph, the time of each peak can be found to see how long it takes 6OCB to reach its K-N, N-I, I-N and N-K phase transitions. These values can be found in Table 5.

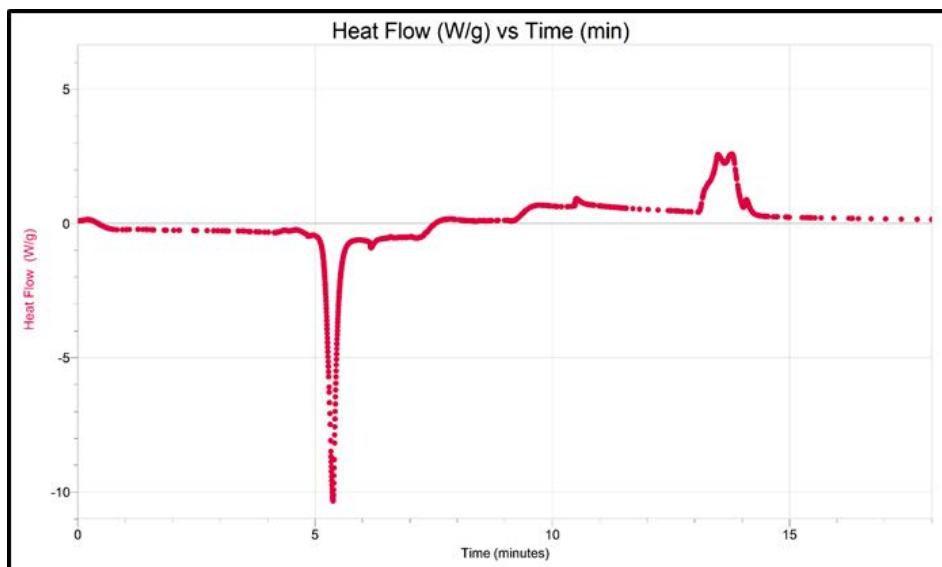


Figure 17: Heat Flow (W/g) vs Time (minutes) of 6OCB Being Heated and Cooled.

All details obtained by analyzing 6OCB DSC data using Logger Pro, as shown in Figures, are given in the data section in Data Tables 1-6.

Data Tables: Details of The Analyzed Data Of 6ocb Can Be Seen Here.

Table 1: Heating and Cooling Phase Transitions of 6OCB.

Sample	Heating				Cooling				
	TKN (°C)	TNI (°C)	ΔH_{KN} (J/g)	ΔH_{NI} (J/g)	TKN (°C)	TNI (°C)	ΔH_{KN} (J/g)	ΔH_{NI} (J/g)	ΔE (J/g)
6OCB	59.55	76.92	159.77	29.33	26.00, 22.54, 18.67	73.94	91.89	33.07	454.5

Table 2: Details of the Heating of 6OCB.

Heating 6OCB										
Transition	Ts (°C)	Te (°C)	TKN/NI (°C)	ΔT (°C)	Cps (J/g°C)	Cpe (J/g°C)	C _{pp} (J/g°C)	C _{pJ} (J/g°C)	ΔC_p (J/g°C)	ΔH (J/g)
K-N	53.98	67.55	59.55	13.57	-1.50	-2.21	-31.01	0.71	29.29	159.77
N-I	72.88	80.34	76.92	7.46	-1.85	-1.78	-2.71	0.07	0.90	29.33

Table 3: Details of the Cooling of 6OCB.

Cooling 6OCB										
Transition	Ts (°C)	Te (°C)	TKN/NI (°C)	ΔT (°C)	Cps (J/g°C)	Cpe (J/g°C)	C _{pp} (J/g°C)	C _{pJ} (J/g°C)	ΔC_p (J/g°C)	ΔH (J/g)
K-N	75.86	68.38	73.94	7.48	1.92	2.09	2.78	0.17	0.81	33.07
N-I	33.18	14.65	26.00, 22.54, 18.67	18.53	1.32	0.81	7.69, 7.75, 2.66	0.51	6.82	91.89

Table 4: Details of Gaussian Analysis from Figures 13 and 14.

	Single Gaussian Peak	Multipeak Gaussian		
		T_KN 1	T_KN 2	T_KN 3
A (J/g°C)	7.348 +/- 0.1778	3.453 +/- 0.1272	6.734 +/- 0.09622	1.595 +/- 0.03316
B (°C)	24.53 +/- 0.05196	25.59 +/- 0.02385	22.75 +/- 0.01426	18.59 +/- 0.01214
C (°C)	4.732 +/- 0.1561	-1.633 +/- 0.08117	2.136 +/- 0.04339	0.8824 +/- 0.02507
D (J/g°C)	0.5724 +/- 0.1825	4.319 +/- 0.1384	1.168 +/- 0.1034	0.9793 +/- 0.02558
Correlation	0.9656	0.9861	0.9986	0.9897
RMSE (J/g°C)	0.6524	0.1853	0.1232	0.08865

Table 5: Time (In Minutes) of Each Phase Transition.

Transition	Heating	Cooling
	Time (min)	Time (min)
K-N	5.38	13.50 (T_KN1), 13.78 (T_KN2), 14.10 (T_KN3)
N-I	6.18	10.52

Table 6: Comparison of the Heating and Cooling of 5CB, 6CB, 5OCB, and 6OCB.

Sample	Molecular Weight (g/mol)	TNI (°C)	CPN (J/g°C)	Nematic Range (°C)	ΔT (°C)	ΔHNI (J/g)
5CB Heat	249.35	35.66	2.097	29.75	18.14	0.37
5CB Cool	249.35	33.55	1.955	15.38	15.48	1.98
6CB Heat	263.38	30.27	1.26	12.82	4.83	0.65
6CB Cool	263.38	26.85	0.41	26.39	6.22	0.98
5OCB Heat	265.35	68.24	3.05	6.31	5.965	26.88
5OCB Cool	265.35	66.56	2.81	41.47	5.746	48.71
6OCB Heat	279.38	76.92	2.71	17.37	7.46	29.33
6OCB Cool	279.38	73.94	2.78	49.94	7.48	33.07

Discussion

In order to understand the behavior of 6OCB in a fuller context, the following figures were created using data from Table 6 to compare the properties of LCs. Figure 18 compares the peak temperatures of the N-I phase transitions of the LCs 5CB, 6CB, 5OCB, and 6OCB. There is a noticeable trend in which the LCs that belong to the nOCB family, 5OCB and 6OCB, reach higher temperatures during their phase transition. This is likely due to the higher molecular weight and strong bonds caused by the oxygen, which require more energy to break down. This energy must be released when cooling, thus, the trend is similar for both heating and cooling.

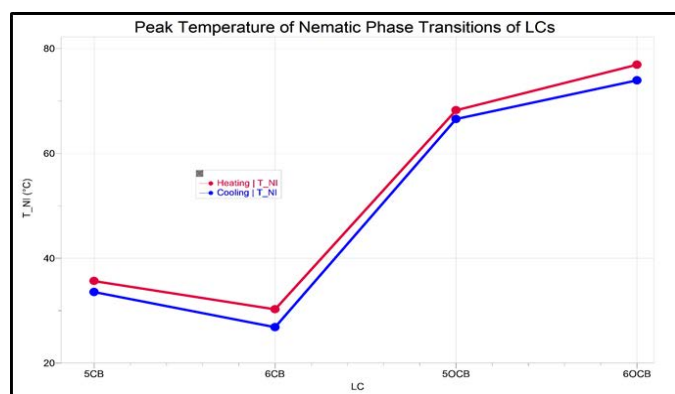


Figure 18: Comparison of the Peak Temperatures of the N-I Transition of 5CB, 6CB, 5OCB, and 6OCB.

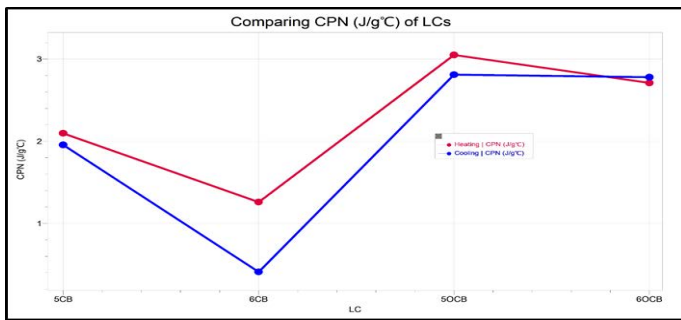


Figure 19: Comparison of the Peak Specific Heat Capacities, CPN (J/g°C), of the N-I Transition of LCs 5CB, 6CB, 5OCB, and 6OCB.

When comparing the specific heat capacities at the N-I peaks, the liquid crystals with an “n” value of 5 seem to have higher heat capacities than their n = 6 counterparts. Additionally, members of the nOCB family have higher specific heat capacities than those of the nCB family of LCs, as shown in Figure 19. The nOCB LCs have higher molecular weights, therefore more energy is required to cause a change in temperature.

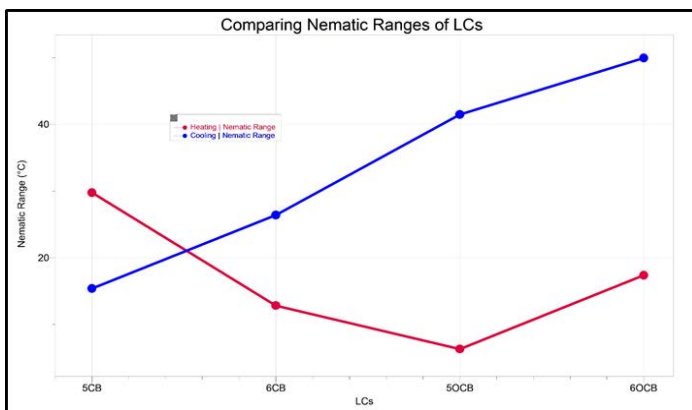


Figure 20: Comparison of the Nematic Ranges (°C) of LCs 5CB, 6CB, 5OCB, and 6OCB.

The nematic ranges of the LCs when being heated and cooled are shown in Figure 20, in order to compare their properties that may be useful for LCD. LCs must be in the nematic state to be utilized in LCD, therefore it is helpful for the LC to remain in this phase for a wide range of temperatures, so it can withstand different environments and changes in weather. The nematic ranges of the LCs while being cooled are higher than the ranges while being heated, with the exception of 5CB, which has the highest range while heated. 6OCB, the focus of this study, has the highest nematic range when being cooled, and has a higher nematic range than 6CB and 5OCB during heating. However, its nematic range while being heated is lower than that of 5CB. Past research has shown that mixing LCs can result in useful properties, changing the temperatures at which phase transitions occur, and increasing nematic ranges [24-28]. It is possible that mixing some 5CB into a sample of 6OCB could show an increase in nematic range, resulting in a material better suited for LCD.

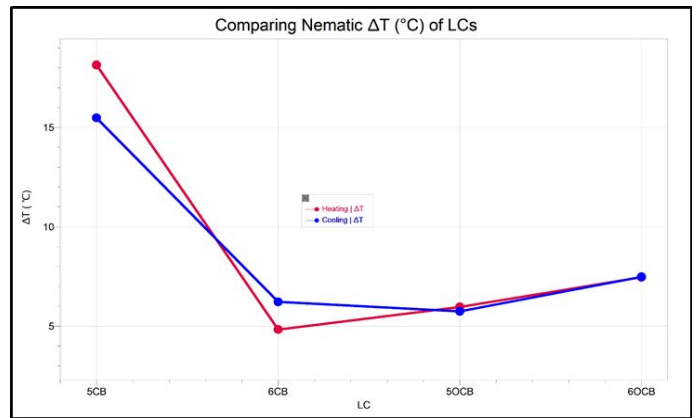


Figure 21: Comparison of the Overall Change in Temperature, ΔT (°C), of the N-I transition of LCs 5CB, 6CB, 5OCB, and 6OCB.

The overall change in temperature for the N-I phase transition, calculated as the difference between T_e and T_s , was highest for 5CB, as seen in Figure 21. There was a similar trend for both heating and cooling, although 6CB has the lowest ΔT while being heated, but 5OCB has the lowest ΔT while being cooled.

The change in internal energy for the N-I phase transition shows a clear trend in Figure 22, as the LCs of the nOCB family have greater enthalpies than those of the nCB family. This difference is likely due to the stronger intermolecular forces present in 5OCB and 6OCB, which have higher molecular weights because of the oxygen, requiring more energy to break and form these bonds.

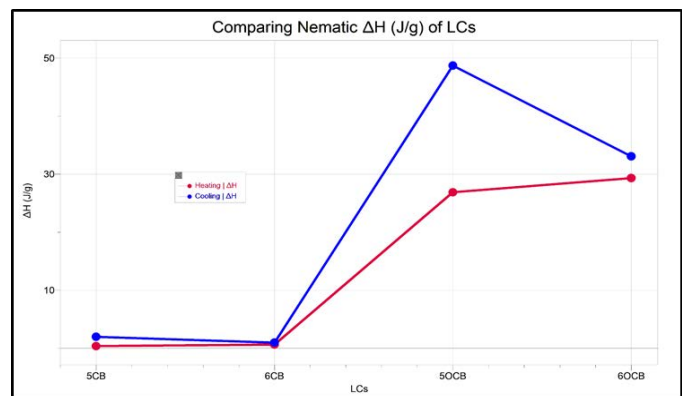


Figure 22: Comparison of the Enthalpy, ΔH (J/g), of the N-I Phase Transition of 5CB, 6CB, 5OCB, and 6OCB.

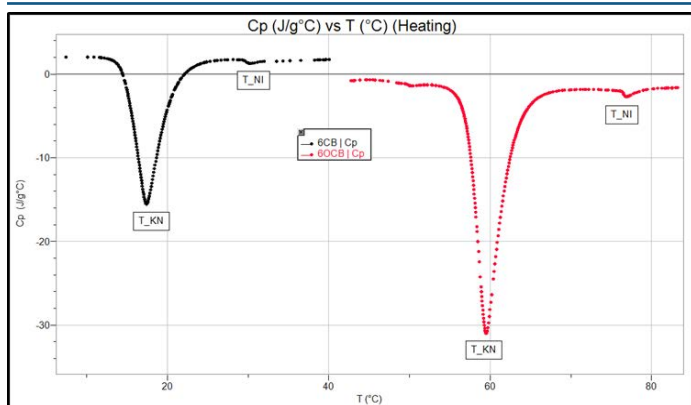


Figure 23: Cp (J/g°C) vs T (°C) of 6CB and 6OCB Undergoing the K-N and N-I Phase Transitions During Heating.

Figure 23 compares the phase transitions of 6CB, in black, and 6OCB, in red, while they are heated. The K-N peak of 6OCB is much larger than the K-N peak for 6CB, as it would take more energy for the substance with a higher molecular weight to undergo a phase transition. 6CB undergoes both transitions at a lower temperature, making its nematic range closer to room temperature. 6OCB has a wider nematic range than 6CB, but it does not reach nematic state until nearly 60 °C. It is possible that mixing 6CB and 6OCB could lower the temperature at which the heating nematic phase occurs, to be more applicable to cooler environments, or to widen the nematic range of the sample.

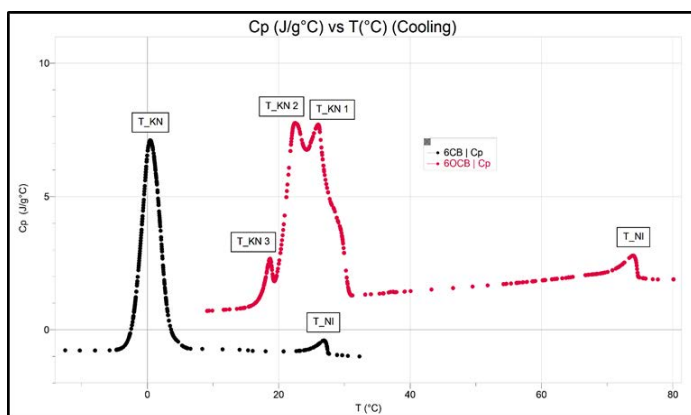


Figure 24: Cp (J/g°C) vs T (°C) of 6CB and 6OCB Undergoing the N-K and I-N Phase Transitions During Cooling.

The behavior of 6OCB while being cooled is compared to that of 6CB in Figure 24. Both LCs have identical molecular structures with the exception of the oxygen atom that connects the head and the tail of 6OCB. It is possible that the presence of this oxygen is responsible for the multi-peaks that appear during the cooling of 6OCB, but not in 6CB. When the molecules are heated, they lose their even spacing, and begin to tangle together, with the oxygen acting like a hook. When the LC is cooled, some molecules are more tangled than others, and reach the crystalline phase at different times, as illustrated by the suggested model, Figure 25. Based on this model, the molecules that are least tangled form the first of the observed exothermic multi-peaks in the N-K transition. After that, the molecules that are somewhat tangled form the second peak. The most tangled molecules take the longest to transition, as the tangled arrangement makes it more

difficult to restore order. These molecules eventually form the third, final peak.

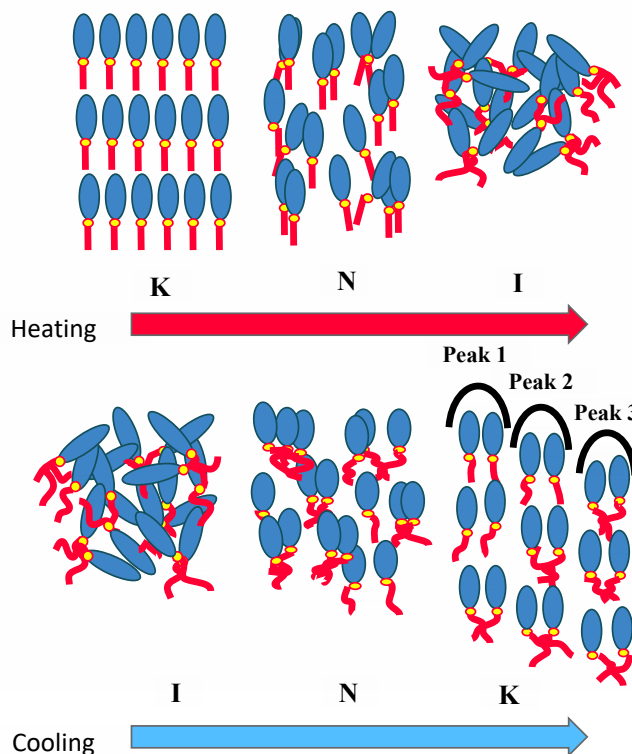


Figure 25: Suggested Model to Explain the Multiphase Crystallization that Occurs in the Cooling of 6OCB.

Conclusion

In this study, the details of the heating and cooling of the liquid crystal 6OCB were examined using DSC. The data collected by DSC was then analyzed in further detail through Logger Pro. Results from this testing were then compared to details of other members of the nOCB family in order to see how the tail length affects an LC's properties. The results were also compared to members of the nCB family in order to explore how the oxygen present in nOCB affects its behavior. It was found that 6OCB has a wide nematic range of 49.94 °C while cooling, which was the largest range out of the LCs that it was compared to. While 5CB had the largest nematic range during heating, 6OCB's range was still larger than that of 6CB and 5OCB. It was also found that 6OCB undergoes both phase transitions at a higher temperature than 6CB, likely due to the presence of oxygen. Furthermore, 6OCB displays unique behavior when it is being cooled from nematic to crystalline, showing multi-peaks that indicate three separate stages of transitioning. The existence of a multi-peak in crystallization can be explained by the model suggested in this paper. This behavior, which does not appear in the cooling of 6CB, suggests that the oxygen atom in 6OCB may facilitate the tangling of the molecules as they cool, with more tangled molecules taking longer to crystallize. The tails of the 6OCB molecules become tangled in three different stages based on their flexibility and speed of cooling, which causes three multi-peaks in cooling. Overall, the wide nematic range of 6OCB while cooling and the temperature at which the nematic phase occurs shows that 6OCB could be useful for LCD in warmer climates. Further research could explore how mixing 5CB or 6CB with 6OCB could widen its nematic range while heating, or possibly

lower the temperature at which the phase occurs.

Acknowledgment

The authors would like to acknowledge Professor John C. MacDonald, Department of Chemistry and Biochemistry, WPI, for helping us with their DSC instrument (Model MDSC 2920 from TA). The student is grateful to Dr. Dipti Sharma for supervising this research internship and manuscript writing during the summer 2023 semester. The authors would also like to thank Emmanuel College for running internship programs for students.

References

1. Slough G (2022) What is Differential Scanning Calorimetry? TA Instruments. From <https://www.tainstruments.com/what-is-differential-scanning-calorimetry/>.
2. Libretexts, Cassabaum, A., Winton V (2023) Differential scanning calorimetry. Chemistry LibreTexts. from [https://chem.libretexts.org/Bookshelves/Physical_and_Theoretical_Chemistry_Textbook_Maps/Supplemental_Modules_\(Physical_and_Theoretical_Chemistry\)/Thermodynamics/Calorimetry/Differential_Scanning_Calorimetry](https://chem.libretexts.org/Bookshelves/Physical_and_Theoretical_Chemistry_Textbook_Maps/Supplemental_Modules_(Physical_and_Theoretical_Chemistry)/Thermodynamics/Calorimetry/Differential_Scanning_Calorimetry).
3. Chiu M H, Prenner E J (2011) Differential scanning calorimetry: An invaluable tool for a detailed thermodynamic characterization of macromolecules and their interactions. *Journal of Pharmacy and Bioallied Sciences* 3: 39.
4. Sharma D, MacDonald J M, Iannacchione G S (2006) Thermodynamics of activated phase transitions of 8CB: DSC and MC calorimetry. *Journal of Physical Chemistry B* 110: 16679-16684.
5. Andrienko D (2018) Introduction to liquid crystals. *Journal of Molecular Liquids* 267: 520-541.
6. Display N V (2018) What is "liquid crystal"? *New Vision Display*. <https://www.newvisiondisplay.com/liquid-crystal/>.
7. Doran M, Seide M, Sharma D (2022) Reporting Strange and Unique Behavior of 4CB Liquid Crystal using Logger Pro. *International Journal of Research in Engineering and Science* 10: 27-41.
8. McDonough K, Vy N C H, Sharma D (2014) Existence of time lag in crystalline to smectic A (K-SmA) phase transition of 4-decyl-4-biphenylcarbonitrile (10CB) liquid crystal. *Journal of Thermal Analysis and Calorimetry* 116: 1515-1520.
9. Seide M, Doran M, Sharma D (2022) Analyzing nematic to isotropic (N-I) phase transition of NCB liquid crystals using Logger Pro. *European Journal of Applied Sciences* 10: 98-124.
10. Sharma D, Farah K (2016) A review of nematic liquid crystals. *Trends in Physical Chemistry* 16: 47-52.
11. What are liquid crystals? Kent State University. <https://www.kent.edu/amhci/what-are-liquid-crystals>.
12. Zhao Y (2005) Thermodynamic and Dynamic Behaviors of Self-Organizing Polymeric Systems [PhD dissertation]. Case Western Reserve University.
13. Mello J, Sharma D (2022) Effect of Reheating and Ramp Rates on Phase Transitions of 5OCB Liquid Crystal using Logger Pro. *International Journal of Research in Engineering and Science*, 10: 218-236.
14. Fisher T (2022) What Is Liquid Crystal Display (LCD)? *Lifewire* <https://www.lifewire.com/what-is-liquid-crystal-display-lcd-2625913>.
15. Kyrnin M (2020) CRT vs. LCD Monitors. *Lifewire* <https://www.lifewire.com/crt-vs-lcd-monitors-833081>.
16. LCD (Liquid Crystal Display). (2019) *WhatIs.com*. <https://www.techtarget.com/whatis/definition/LCD-liquid-crystal-display>.
17. Tyson J (2023) How LCDs work. *HowStuffWorks*. <https://electronics.howstuffworks.com/lcd.htm#:~:text=LCDs%20use%20these%20liquid%20crystals,as%20either%20thermotropic%20or%20lyotropic>.
18. Tyson J, Carmack C (2023) How Computer Monitors Work. *HowStuffWorks*. <https://computer.howstuffworks.com/monitor5.html>.
19. Lorch M (2022) The chemistry behind your LCD flat-screen devices: how a scientist changed the world. University of Hull from <https://www.hull.ac.uk/work-with-us/more/media-centre/news/2022/the-chemistry-behind-your-lcd-flat-screen-devices-how-a-scientist-changed-the-world>.
20. Sharma D, Tiwari G, Tiwari S N (2021) Electronic and electro-optical properties of 5CB and 5CT liquid crystal molecules: A comparative DFT study. *Pramana* 95. <https://doi.org/10.1007/s12043-021-02114-z>.
21. Mello J, Sharma D (2022) Details of Nematic Phase Transition and Nematic Range of 5OCB Liquid Crystal using Logger Pro. *International Journal of Research in Engineering and Science*, 10: 197-217.
22. Ge Y, Dai J, Qian K, Hepburn D, Zhou C (2015) Simulation of domestic electricity load profile by multiple Gaussian Distribution. *23rd International Conference on Electricity Distribution* 0107.
23. Sharma D, Sharma O, MacDonald J, Kumar A, Gupta R, et al. (2023) Reporting Three Unique "Induced Glass Transitions" (IGTs) Appeared in GeSSb Glassy Alloys using DSC. *International Journal of Engineering Inventions* 12: 27-39.
24. Doran M, Sharma D (2023) Effect of Ramp Rates on Phase Transitions of a Next Generation "Binary Liquid Crystal System" (BLCS) 5CB+7CB. *International Journal of Engineering Inventions* 12: 291-306.
25. Doran M, Sharma D (2022) Melting and Nematic Phase Transitions of a Next Generation "Binary Liquid Crystal System (BLCS)" 5CB+7CB using Logger Pro. *International Journal of Research in Engineering and Science*, 10: 462-483.
26. Özgün Ş, Okumuş M (2011) Thermal and Spectrophotometric Analysis of Liquid Crystal 8CB/8OCB Mixtures. *Brazilian Journal of Physics* 41: 118-122.
27. Seide M, Sharma D (2023) Observance of Multiple Melting and Nematic Phase Transitions in A Next Generation "Quaternary Liquid Crystal System" (QLCS). *Global Journal of Materials Science and Engineering* 5.
28. Seide M, Sharma D (2023) Reporting Phase Transitions of a New Generation "Tertiary Liquid Crystal System" (TLCS) using Logger Pro. *SSRG International Journal of Applied Physics* 10: 22-33.

Copyright: ©2023 Dipti Sharma, et al. This is an open-access article distributed under the terms of the Creative Commons Attribution License, which permits unrestricted use, distribution, and reproduction in any medium, provided the original author and source are credited.